Laser Induced Fluorescence Measurement of Ion Temperatures in Argon Flux Ropes

Corey Adams, Walter Gekelman, Bart Van Compernolle
University of California, Los Angeles
(Dated: August 25, 2010)

ABSTRACT

This paper describes the measurements of ion temperatures in an argon plasma experiment. Three flux ropes were created in a quiet background plasma, and the method of laser induced fluorescence was used to map temperature gradients of the three flux ropes at different times. Ion temperatures were observed in the 1 - 6 eV range, and the heat diffused due to the gyro-radius of argon ions.

INTRODUCTION

Magnetic flux ropes have been a topic of interest in plasma physics for at least a decade. In highly conducting fluids it is proven mathematically that the magnetic fields become attached to the medium (frozen in condition), and plasmas are a medium where this phenomenon readily occurs. In some cases of strong electric currents in the plasma, the magnetic fields become rope like inside the current channels, leading to the formation of magnetic flux ropes.

Flux ropes are observed in nature in various situations. Flux ropes have been observed as a result of coronal mass ejections [1], and these flux ropes can reach from the sun as far as the earth and back. Flux ropes also exhibit interesting properties as dynamical systems because they interact via $j \times B$ forces. The helical B-fields surrounding the flux ropes move with the ropes, causing phenomenon such as magnetic reconnection.

This paper presents results of an experiment designed to measure ion temperatures of a magnetic flux rope configuration. Laser Induced Fluorescence was used on three flux ropes in an argon plasma, created in the Large Plasma Device at UCLA's Basic Plasma Science Facility.

Laser Induced Fluorescence (LIF) works by exciting a transition in argon ions and observing the emission at another wavelength. By assuming the ions are distributed in a normal distribution, and using the properties of the Doppler shift, temperatures of ions can be spatially determined.

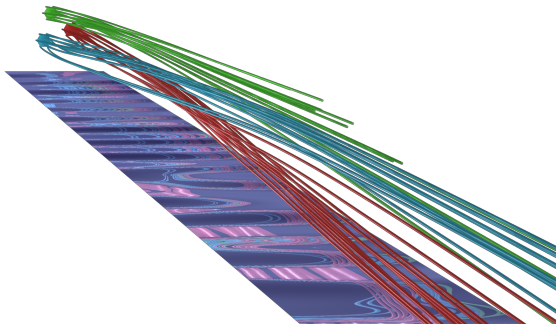

FIG. 1: Magnetic flux ropes created in the Large Plasma Device at UCLA. The flux ropes (field lines traced from a 3D data set) are colored to distinguish them.

LASER INDUCED FLUORESCENCE

Laser induced fluorescence is a diagnostic tool used to measure properties of the ions in plasma, in particular ion temperatures. To perform laser induced fluorescence, a transition level in Argon ions was stimulated, and detected by the resultant emission of a photon due to the decay. By observing the emission as a function of the frequency of the stimulating light, and by using the doppler shift, a Distribution function of the ions is measured. With knowledge of the distribution function, the temperature of the ions can be determined (assuming the line broadening mechanism is Doppler broadening).

Laser Induced Fluorescence is a scheme presented as early as 1975 by Stern and Johnson [2], and has been used for diagnostics in plasmas since. [3] [4] [5] The scheme used in this experiment was adapted from [3].

In figure 2, the energy level diagram of argon ions used in this laser induced fluorescence measurement are shown. The 3D state is metastable, with a lifetime of over a millisecond [6]. Therefore, the 3D state will be populated due to collisions with energetic electrons in the tail of the electron distribution.

To induce fluorescence, a laser is tuned to have the energy required to excite the electron to another energy level. This excites electrons in the 3D state to the 4P state, and from there they decay to the 4S state. The probability of that decay occurring is .665 [7], and so a significant portion of the electron decays are to the 4S state. When they decay, the ions emit a photon of wavelength 461nm; this is the induced fluorescence that is detected.

The energy transition from the 3D to the 4P is narrow enough that ions moving with sufficient velocity towards or away from the incident laser see doppler shifted laser light and will not absorb it. The frequency shift is given by $\Delta\nu = \nu_o v/c$, where ν_o is the frequency in the rest frame of the laser. By scanning the laser over a range

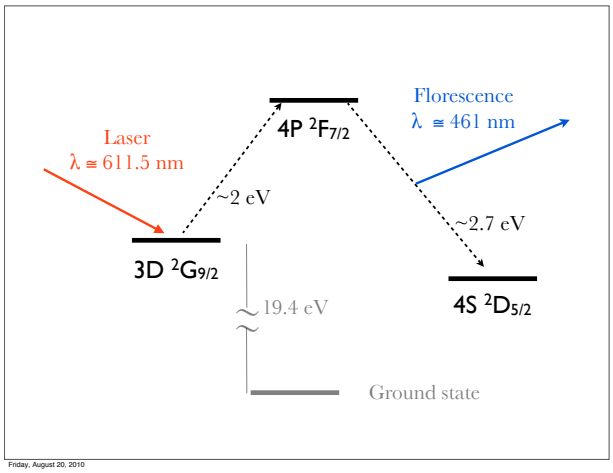

FIG. 2: Energy Levels relevant to laser induced fluorescence.

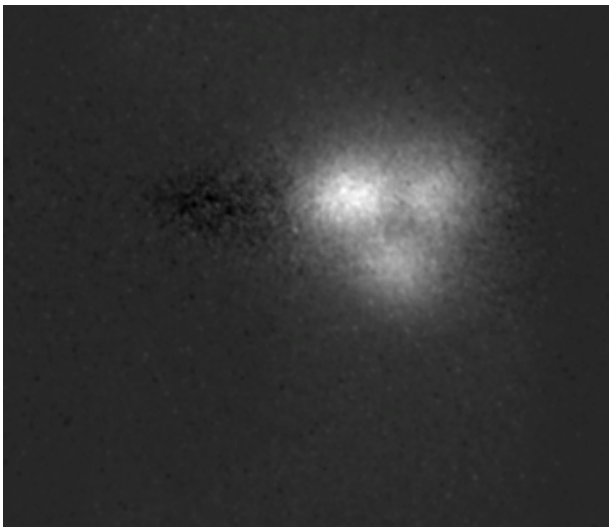

FIG. 3: A picture of LIF emission at a single stimulating wavelength. The three bright spots are the three flux ropes.

of frequencies ($\nu_a \leq \nu_o \leq \nu_b$), moving ions are caused to absorb and fluoresce as well (of course, the only ion velocity component that matters is the one parallel to the laser light).

At each wavelength of light incident onto the ions, the fluorescence intensity changes depending on how many ions are moving with the appropriate velocity to absorb. By recording the level of fluorescence at each point in the sheet of light and for each wavelength, a number proportional to the amount of ions moving with a certain calculable velocity at each point is obtained. This data, when combined over the whole range of velocities, produces a Maxwell distribution function,

$$f = Ae^{\frac{-M_i v^2}{2kT_i}}, \tag{1}$$

where M_i is the mass of argon ions, and T_i is the ion temperature, and A is a constant dependent on plasma density. This function can be written in units of frequency, so that it gives the number of atoms moving with the velocity resonant with the doppler shifted frequency. By making the change of variables according to the Doppler shift of light, $v \rightarrow c\Delta\nu/\nu_o$, the distribution becomes dependent on the frequency of the laser:

$$f = Ae^{\frac{-M_i c^2(\Delta\nu)^2}{2kT_i(\nu_o)^2}}. \tag{2}$$

The distribution above has a full width at half maximum dependent on the temperature of the ions. The standard deviation of the function is given by

$$\sigma_\nu = \frac{\nu_o}{c}\sqrt{\frac{kT_i}{M_i}}. \tag{3}$$

The standard deviation, when divided by the central frequency ν_o, becomes dependent only on temperature. Thus the standard deviation measured in wavelength, divided by the central wavelength, is equal to the standard deviation in frequency divided by the natural frequency: $\sigma_\nu/\nu_o = \sigma_\lambda/\lambda_o$. The standard deviations are numerically calculated from collected data, and the temperature is then calculated from equation 3.

MEASURING MAGNETIC FLUX ROPES

Magnetic flux ropes have been studied using the Large Plasma Device at the Basic Plasma Science Facility at the University of California, Los Angeles [8], [9]. For this experiment, three 2.5 cm diameter flux ropes were emitted from a lanthanum hexaboride (LaB_6) cathode and end 9 meters away on a mesh anode. Laser induced fluorescence is performed by shining a sheet of light into a cross section of the flux rope experiment.

The fluorescencent light is emitted in 4π steraradians, so a mirror is placed further down the machine and light reflected into a CCD camera. The laser pulse lasts ~8.5ns, the fluorescence lasts ~10ns [6], and the camera is set for an exposure of 20 nanoseconds. Due to the noise inherent to the experiment (the LIF signal is weak), an average of 300 shots per wavelength is taken to produce a good signal to noise ratio. The background flux ropes also emit light at 461nm. To isolate the Laser Induced Fluorescence signal the average of the data without laser input was digitally subtracted and an LIF signal with a signal to noise ratio of 20 was obtained. Figure 3 shows CCD image at a wavelength where a clear LIF signal can be seen due to flux ropes.

By taking data over a range of incident wavelengths (611.52 to 611.62 nm), at each pixel a function such as the one seen in figure 4 is constructed. The data collected

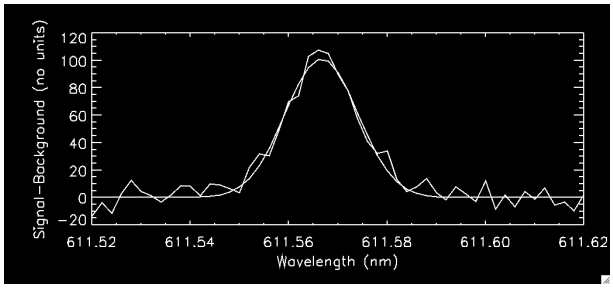

FIG. 4: The observed camera intensity at a fixed pixel of LIF signal data, with a gaussian fitted to the data. The width of the graph is used to determine the temperature. The vertical units are arbitrary.

is gaussian, as seen by comparison to the gaussian fit, also in figure 4. The width of the peak is used to determine the temperature at each pixel.

EXPERIMENTAL RESULTS

LIF data was collected in at 3 different times. The flux ropes were initiated at $t = 0$ and the data acquired at 20, 100, and 200 microseconds later. The observed temperatures ranged from about 1 (background plasma) to 6 eV. It is interesting to note that very soon after the flux ropes turn on, the heating becomes widespread and encompasses all of the flux rope region.

At t = 20 microseconds, the flux rope configuration can still be seen in the pattern of the heating; there are three distinct peaks in the temperature map, corresponding to the three rope configuration. At 100 and 200 microseconds, the heat is more spatially spread out, as seen in figure 5. Conversely, as seen in figure 6, even at times when the ion temperature has spread over an area greater than that encompassed by the flux ropes, the electron temperature remains confined to the flux ropes

The majority of the heating is most likely due to resistive heating from the electron current flowing through the plasma. The electrons and ions collide via Coulomb interactions, which transfers energy from the electron current to the ions. From the heat distribution at 20 microseconds, it seems reasonable that this heating takes place at the location of the three beams, as would be expected.

The heating likely spreads out due to the increasing gyro-radius of the argon ions ($r_g = mv/qB$). At temperatures of 5 eV and a magnetic field of 900 Gauss, there are a significant number of ions with gyro-radius greater than 2.5 cm, which is the diameter of each flux rope. Thus, as ions are heated they leave the flux ropes due to their gyro-rotation; this is what causes the diffusion of the heat of the ions. The electrons have a much smaller gyro-radius due to their smaller mass, and are more likely to stay confined to the flux ropes ($r_e \approx 100\mu m$). Figure 6 shows that the electron temperature has not diffused like the ion temperature, even at 200 microseconds.

It is worthwhile to consider how long the plasma takes to equilibrate thermally. According to [10], the self-collision time for a species in a plasma is given by

$$t_c \approx \frac{T^{3/2}}{Z^4 n}(\frac{m}{m_p})^{1/2} \times 10^6 \qquad (4)$$

in seconds, where T is the plasma temperature in Kelvin, Z is the charge number, m is the mass of the species in question, n is the density, and m_p is the proton mass. For the argon ions in this experiment, this number was on the order of 100 microseconds. However in this experiment the electrons in the current channels associated with the flux ropes are heated first. The relevant time is ion-electron equilibration time. This time is given, theoretically, as

$$t_{eq} \approx \frac{\sqrt{2} m_i m_e \pi^{3/2} k^{3/2} \epsilon_o^{3/2}}{10 q_i^2 q_e^2 n_i}(\frac{T_e}{m_e} + \frac{T_i}{m_i})^{3/2}. \qquad (5)$$

When calculated, this time is about 10 milliseconds for electron-ion thermal equilibration. This does not agree with the observed results because the ions are being heated on much faster time scale than 10 milliseconds. While the cause of the heating is unknown, it is possible that it is due to plasma turbulence as well as coulomb scatterings.

CONCLUSION AND ACKNOWLEDGEMENTS

In this experiment laser induced fluorescence was successfully used to determine ion temperatures in magnetic flux ropes in argon. Ion temperatures peaking in the 6 eV range, with heat diffusion occurring due to the gyro-radius of the argon ions exceeding the diameter of the flux ropes was observed.

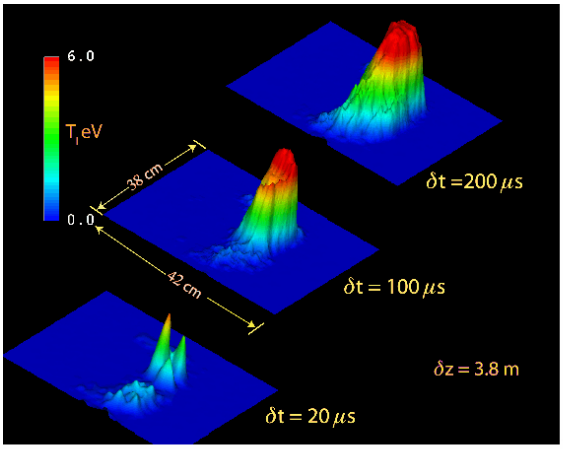

FIG. 5: Ion temperatures as measured 20, 100 and 200 μs after the flux ropes begin.

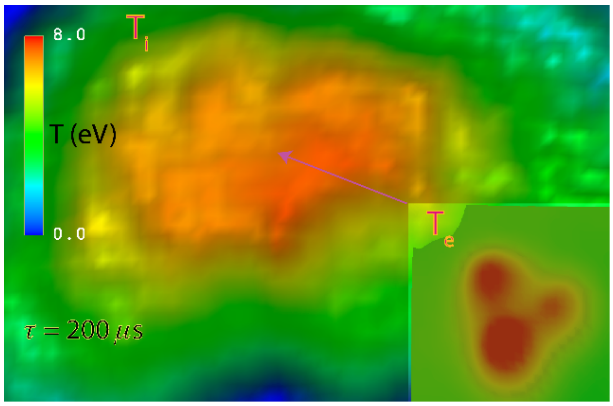

FIG. 6: Ion and electron (inset) temperatures at 200 μs after the flux ropes turn on.

The author would like to thank Walter Gekelman and Bart Van Compernolle for their mentoring and assistance during this experiment. Also, Mio Nakamoto for her help in running the experiment and the Natural Science Foundation for funding the UCLA Research Experience for Undergraduates program. This work was done at the Basic Plasma Science Facility which is funded by the Department of Energy and the Natural Science Foundation.

[1] J. Chen, R. A. Howard, G. Brueckner, R. Santoro, J. Krall, S. E. Paswaters, O. C. S. Cyr, R. Schwenn, P. Lamy, and G. M. Simnett, The Astrophysical Journal **490** (1997).
[2] R. Stern and J. J. III, Physical Review Letters **34** (1975).
[3] B. Jacobs, W. Gekelman, P. Pribyl, and M. Barnes, Physical Review Letters **105** (2010).
[4] F. Anderegg, R. A. Stern, F. Skiff, B. A. Hammel, M. Q. Tran, P. J. Paris, and P. Kohler, Physical Review Letters **57** (1986).
[5] R. M. ad J. P. Booth, E. A. Hudson, J. Thomas, and D. Zimmerman, This Solid Films **515** (2007).
[6] M. Goeckner and J. Goree, Journal of Vacuum Science Technology (1988).
[7] G. Severn, D. Edrich, and R. McWilliams, Review of Scientific Instruments **69** (1998).
[8] E. E. Lawrence and W. Gekelman, Physical Review Letters **103** (2009).
[9] S. Tripathi and W. Gekelman, Physical Review Letters **105** (2010).
[10] G. Schmidt, *Physics of High Temperature Plasmas: An Introduction* (Academic Press Inc, 1966).